Biochimica et Biophysica Acta 1832 (2013) 2009–2018

Contents lists available at ScienceDirect

Biochimica et Biophysica Acta

journal homepage: www.elsevier.com/locate/bbadis

Glutathione peroxidase contributes with heme oxygenase-1 to redox balance in mouse brain during the course of cerebral malaria

María Linares [1,2], Patricia Marín-García [1,3], Gabriela Martínez-Chacón, Susana Pérez-Benavente, Antonio Puyet, Amalia Diez, José M. Bautista *

Departamento de Bioquímica y Biología Molecular IV and Instituto de Investigación Hospital 12 de Octubre, Universidad Complutense de Madrid, Ciudad Universitaria, 28040 Madrid, Spain

ARTICLE INFO

Article history:
Received 25 January 2013
Received in revised form 9 July 2013
Accepted 10 July 2013
Available online 18 July 2013

Keywords:
Oxidative stress
Experimental cerebral malaria
Redox proteomics
Redox balance

ABSTRACT

Oxidative stress has been attributed both a key pathogenic and rescuing role in cerebral malaria (CM). In a *Plasmodium berghei* ANKA murine model of CM, host redox signaling and functioning were examined during the course of neurological damage. Host antioxidant defenses were early altered at the transcriptional level indicated by the gradually diminished expression of superoxide dismutase-1 (*sod-1*), *sod-2*, *sod-3* and catalase genes. During severe disease, this led to the dysfunctional activity of superoxide dismutase and catalase enzymes in damaged brain regions. Vitagene associated markers (heat shock protein 70 and thioredoxin-1) also showed a decaying expression pattern that paralleled reduced expression of the transcription factors Parkinson disease 7, Forkhead box O 3 and X-box binding protein 1 with a role in preserving brain redox status. However, the oxidative stress markers reactive oxygen/nitrogen species were not accumulated in the brains of CM mice and redox proteomics and immunohistochemistry failed to detect quantitative or qualitative differences in protein carbonylation. Thus, the loss of antioxidant capacity was compensated for in all cerebral regions by progressive upregulation of heme oxygenase-1, and in specific regions by early glutathione peroxidase-1 induction. This study shows for the first time a scenario of cooperative glutathione peroxidase and heme oxygenase-1 upregulation to suppress superoxide dismutase, catalase, heat shock protein-70 and thioredoxin-1 downregulation effects in experimental CM, counteracting oxidative damage and maintaining redox equilibrium. Our findings reconcile the apparent inconsistency between the lack of oxidative metabolite build up and reported protective effect of antioxidant therapy against CM.

1. Introduction

Malaria caused by *Plasmodium falciparum* has the highest rates of mortality in children because of its most life-threatening complication cerebral malaria (CM). This is an acute neurological condition characterized by seizures, metabolic acidosis, hypoglycaemia and coma [1]. CM has a mortality rate of 10–14% and causes around 600,000 annual deaths among young children predominantly in sub-Saharan Africa and Southeast Asia [2]. Moreover, child survivors often show long-standing neurocognitive sequelae, particularly in Africa [1,3].

Prior studies have attributed an important role in CM development to an altered redox equilibrium. Some authors have suggested that reactive oxygen species (ROS), produced by both host and parasite, accumulate during the development of this acute neurological condition promoting oxidative stress [4–6]. The increased production of free radicals (e.g. superoxide anion and hydroxyl radical) has been observed in activated leucocytes, in endothelial cells during the adhesion of parasitized red blood cells (pRBC) and, most strikingly, during hemoglobin digestion in the parasite food vacuole [4,7–9]. This, in turn, causes protein oxidation in the parasite and host membranes [10,11]. Indeed, enhanced host ROS production during the course of CM is thought to play both a beneficial and pathological role depending on the amount and place of release. Beneficial ROS effects contest parasite growth whereas prolonged ROS exposure could cause cell damage in the host brain [4,5]. In addition, several antioxidant treatments have shown protection against experimental cerebral malaria (ECM) and prevention of persistent cognitive damage [6,12,13], suggesting the failure of host antioxidant mechanism during CM. Notwithstanding, some studies have failed to observe ROS accumulation and oxidative stress in brain during CM [14], questioning the role played by these molecules in the pathogenesis of this disease [8].

* Corresponding author at: Dpto. Bioquímica y Biología Molecular IV, Universidad Complutense de Madrid, Ciudad Universitaria, 28040 Madrid, Spain. Tel.: +34 91 394 3823; fax: +34 91 394 3824.
E-mail address: jmbau@ucm.es (J.M. Bautista).
[1] M.L. and P.M.G. contributed equally to this work and should be considered first authors.
[2] Present address: Diseases of the Developing World, GlaxoSmithKline, 28760 Tres Cantos, Madrid, Spain.
[3] Present address: Department of Preventive Medicine, Public Health and Medical, Immunology and Microbiology, Faculty of Health Sciences, Rey Juan Carlos University, Alcorcón, Madrid, Spain.

0925-4439/$ – see front matter © 2013 Elsevier B.V. All rights reserved.
http://dx.doi.org/10.1016/j.bbadis.2013.07.010

Intra and extracellular antioxidant defenses exist in the host to prevent oxidative stress, whereby the superoxide radical is reduced by superoxide dismutase (SOD) to hydrogen peroxide, which is reduced to water by both catalase (CAT), a peroxisomal enzyme with a central function in brain cells, and glutathione peroxidase (GPX) [15]. Moreover, brain cells overcome oxidative stress through additional antioxidant pathways such as those involving heat shock proteins (HSP), heme oxygenase (HO), and thioredoxin (TRX) [16].

In the present study, we examined the state of these host antioxidant defenses and their role in oxidative damage during the course of the disease in a mouse ECM model. Here we report the dysfunction of several host antioxidant systems associated with the reduced expression of transcription factors involved in preserving brain host redox status. Oxidative stress markers failed to accumulate in brain regions in parallel with the compensatory induction of two major antioxidant enzymes. Our results reconcile the controversial idea of a lack of oxidative stress build up with the known protective effect of antioxidant therapy against CM.

2. Materials and methods

2.1. Induction of malaria in mice and disease assessment

All experiments involving animals were conducted at the Universidad Complutense de Madrid in accordance with national and international guidelines for animal care. The study protocol was approved by the Animal Experimentation Committee of the Complutense University at its meeting on February 11th 2011.

We used 44 five-weeks-old male C57BL/6 mice, as a CM susceptible strain and 20 five-weeks-old male BALB/c mice, as a non-susceptible CM model. The animals were purchased from Harlan Ibérica (Barcelona, Spain) and housed under standard conditions and supplied with food and water ad libitum. In 32 C57BL/6 mice, CM was induced by intraperitoneal injection of 5×10^6 *P. berghei* ANKA pRBC, as previously described [17]. In a separate experiment 10 BALB/c mice were injected with a similar number of *P. berghei* ANKA pRBC. Uninfected mice were used as controls in both experiments. Our choice of using non-injected animals was based on the national and international regulations regarding animal experimentation implemented at our University by the Committee of Animal Experimentation aimed at minimizing animal suffering. According to previous findings and reports [17,18], injected and non-injected control mice show identical behavior and histological phenotype during the experimental course, with no signs of disease or distress.

The infected C57BL/6 mice developing CM were monitored daily by inspection of clinical signs and classified into 4 clinical stages using the method of clustering animals by neurological symptoms as previously described [17]. BALB/c mice were sacrificed when reaching the same range of parasitemia than C57BL/6 mice. After their sacrifice by cervical dislocation, the olfactory bulb, frontal cortex, hippocampus, thalamus–hypothalamus, cerebellum and brainstem were immediately removed.

2.2. Mouse antioxidant system and transcription factor expression assays

Antioxidant molecules and transcription factors (TF) mRNA levels in olfactory bulb, frontal cortex, hippocampus, thalamus–hypothalamus, cerebellum and brainstem were determined by quantitative reverse transcriptase PCR (qRT-PCR) as previously described [18]. Specific primers and probes for *sod-1*, *sod-2*, *sod-3*, *gpx-1*, *cat*, *trx-1*, *ho-1*, *hsp70*, Parkinson disease 7 (*park7*), Forkhead box O 1 (*foxo1*), *foxo3*, X-box binding protein 1 (*xbp1*) and the house keeping *β-actin* genes (Assays-on-Demand™ Gene Expression products, TaqMan MGB probes, Applied Biosystems, Warrington, UK) were used. The specificity of the primers and probes used was verified by basic local alignment search tool (BLAST) analysis, comparing the mouse genes selected with the *P. berghei* genome and no significant similarity was found. The *β-actin* gene served as an endogenous control to check for any slight variation in the initial concentration, the total RNA quality and the conversion efficiency of the reverse transcription reaction.

N-fold changes were calculated by expressing the amount of mRNA for each molecule present in each mouse vs. the mean amount of mRNA for the molecule detected in control mice.

2.3. CAT, SOD and GPX enzyme activity

100 μg of total brainstem and cerebellum protein extract from the different groups of animals were loaded onto a 15% or 8% native acrylamide gel (for SOD and GPX or CAT activity, respectively) in Tris–glycine running buffer and run at 120 V. Enzyme activities were visualized as described previously [19–21] as clear bands against a dark background. In all assays, protein loading was determined by Coomassie Brilliant Blue staining. Bands were quantified using Quantity-One 1-D analysis software (Bio-Rad Laboratories Inc., Munich, Germany). Relative optical density was calculated as the normalized enzyme activity in each mouse relative to the mean value obtained in control mice.

2.4. Reactive oxygen species/reactive nitrogen species (RNS)

Cerebella and brainstems from animals at stage IV of CM were homogenized in cold phosphate buffer and total ROS/RNS contents were determined using the OxiSelect™ In Vitro ROS/RNS Assay Kit (Cell Biolabs, Inc., San Diego, USA) following the manufacturer's instructions.

2.5. Protein carbonylation

2.5.1. Oxyblot analysis

Protein from control and CM cerebella was extracted and derivatized before 2D electrophoresis as previously described [22]. Derivatized proteins were precipitated using trichloroacetic acid (TCA)-acetone and resuspended in a buffer containing 7 M urea, 2 M thiourea, 4% 3-[(3-cholamidopropyl) dimethylammonio]-1-propanesulfonate (CHAPS), 0.5% MEGA-10, and 10 mM dithioerythritol.

Proteins were cup-loaded onto immobilized pH gradient (IPG) strips (pH 3–11 NL, 18 cm) that had been previously hydrated overnight in a buffer containing 7 M urea, 2 M thiourea, 4% CHAPS, 1.2% DeStreak and 0.5% ampholytes, pH 3–11. First-dimensional separation was by isoelectric focusing (IEF) using the IPGphor 3 IEF system (GE Healthcare, Buckinghamshire, UK) at 20 °C. The voltage was gradually ramped: 3 h 300 V, 6 h 300–1000 V, 3 h 1000–8000 V, and a final step-n-hold at 8000 V for the next 7 h. The run was terminated after ~70,000 V h. The focused strips were equilibrated in equilibration solution (50 mM Tris 8.8, 6 M urea, 30% glycerol, 2% sodium lauryl sulfate (SDS)) containing 1% dithiothreitol reducing agent for 10 min, and transferred to 4% iodoacetamide equilibration solution for a further 10 min. The second-dimension SDS-PAGE was run on homogeneous 12.5% T and 2.6% C casted polyacrylamide gels. Electrophoresis was carried out at 4 °C, 2 W overnight using two Hoeffer units. For each experimental condition (CM or control), 4 gels were run in parallel under identical 2D electrophoresis conditions. Two gels were stained with Sypro Ruby to visualize total proteins and the other two gels were used for subsequent carbonyl modified protein detection. These two gels prepared for CM and control animals were transferred to polyvinylidene fluoride (PVDF) membranes and transfer efficiency was confirmed by: (i) gel staining with Sypro Tangerine before transfer and (ii) membrane staining with Sypro Ruby. Any potential interference of Sypro Tangerine during immunodetection was previously discarded. Carbonyl groups in the transferred membranes containing derivatized proteins were immunodetected as previously described [22] using the anti-2,4-dinitrophenylhydrazone (DNP) primary antibody (1/10,000, Sigma, Saint Louis, USA). Gel and immunoblot images were analyzed using Quantity-One 1-D and PDQuest analysis software (BioRad Laboratories Inc., Munich, Germany). The total amount

of protein carbonylation was normalized to total protein content and referred to the mean value obtained in control mice.

2.5.2. Immunohistochemistry

Control and infected mice were sacrificed and whole brains removed and subjected to a cryoprotection process. 10-μm sagittal sections of brain tissue were cut using a Leica 3050 M cryostat and incubated as described previously [23]. Specific detection of protein carbonylation was done by indirect peroxidase staining using the Elite Vectastain kit (Vector Laboratories, Peterborough, UK) following the manufacturer's instructions. Chromogen reactions were performed with diaminobenzidine (Sigma, Saint Louis, USA) and 0.003% hydrogen peroxide for 10 min. Finally brain sections were coverslipped with Fluorsave™ Reagent. Images were captured with Olympus DP50 digital camera equipped to microscope Olympus BX50 using Studio Lite computer.

2.6. Western blot analysis

Total tissue protein was extracted from the brainstem and cerebellum of the different groups of animals. 10 μg of each protein extract were separated on a 10% SDS-acrylamide gel and transferred to nitrocellulose membranes and then blocked for 1 h using phosphate buffer-Tween 0.05% solution containing 5% non fat skimmed milk. Next, the commercial polyclonal antibodies anti-HO-1 (1/1000, Assay Designs, Ann Arbor, MI; Enzo Life Sciences Inc., Lausen, Switzerland) or anti-glyceraldehyde 3-phospate dehydrogenase (GADPH) (1/10,000, Applied Biosystems, Warrington, UK) were probed overnight at 4 °C. Finally, membranes were incubated 1 h at room temperature with horseradish peroxidase-conjugated anti-rabbit or anti-mouse IgG (1/5000, GE Healthcare, Buckinghamshire, UK) and visualized by the ECL method (SuperSignal West Pico Chemiluminescent Substrate Thermo Scientific, Rockford, USA). Chemiluminescence images were quantified by densitometry using Quantity-One 1-D analysis software (Bio-Rad Laboratories Inc., Munich, Germany). Relative optical density was calculated as the normalized expression of the enzyme in each mouse relative to the mean value obtained in control mice.

2.7. Statistical analysis

Data are presented as the mean ± standard deviation. The Mann Whitney *U* and Kruskal–Wallis non-parametric tests were used to compare two or more groups respectively. Analyses were performed independently for each molecule and region. All statistical tests were performed using the SPSS 15.0 statistics package. The level of significance was set at a $P \leq 0.05$.

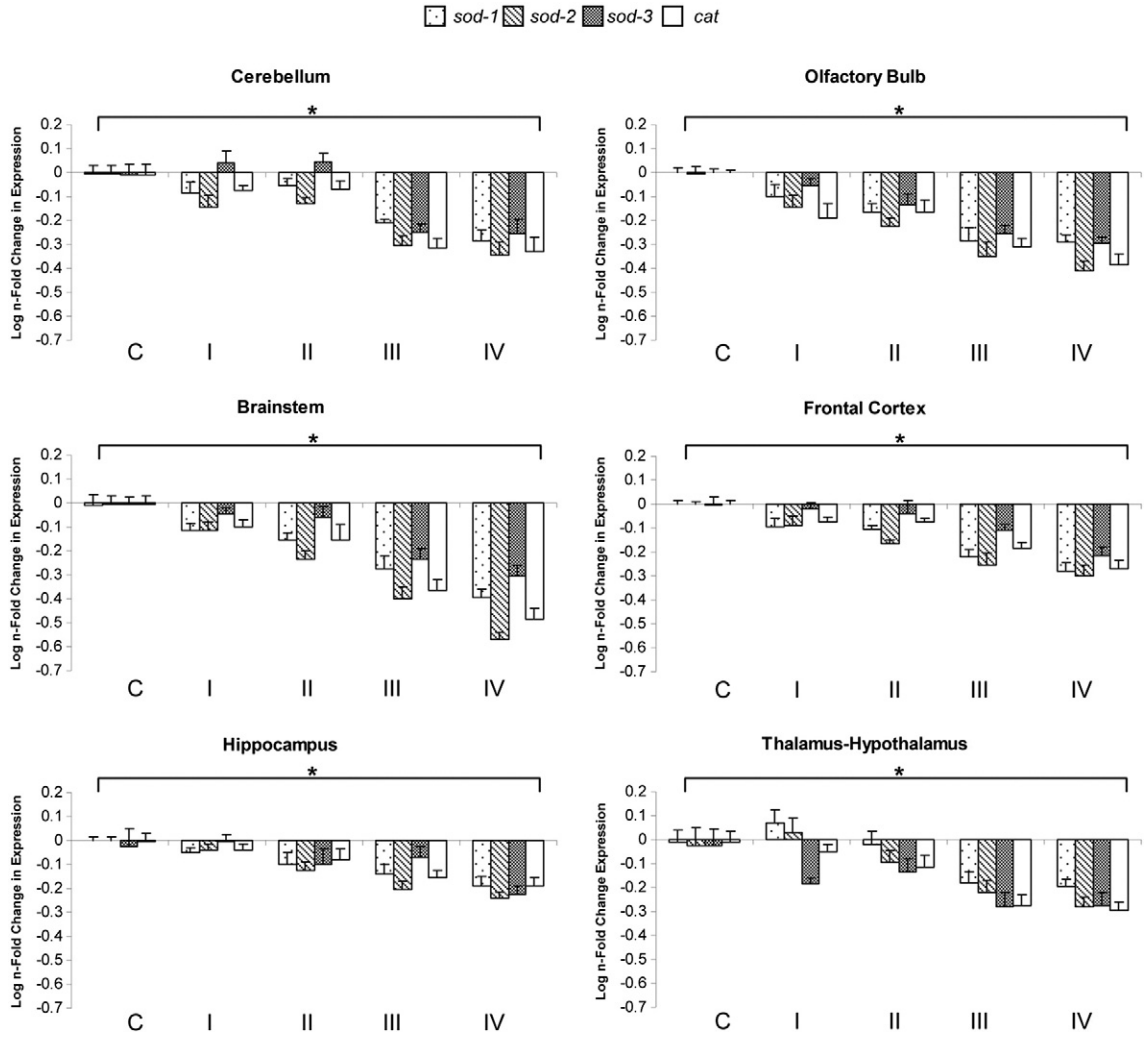

Fig. 1. Expression of *sod* and *cat* mRNA. *sod-1*, *sod-2*, *sod-3* and *cat* mRNA levels in the cerebellum, olfactory bulb, brainstem, frontal cortex, hippocampus and thalamus–hypothalamus detected in control (C) and CM mice at different disease stages (I–IV). Data are the mean ± standard error of determinations in 5–7 animals. *P* values for significant differences observed in the cerebellum: *sod-1*, *sod-2*, *cat*, $P \leq 0.001$; *sod-3*, $P \leq 0.005$; olfactory bulb: *sod-1*, *sod-2*, *sod-3*, *cat*, $P \leq 0.001$; brainstem: *sod-1*, *sod-2*, *sod-3*, *cat*, $P \leq 0.001$; frontal cortex: *sod-1*, *sod-2*, *cat*, $P \leq 0.001$; *sod-3*, $P \leq 0.005$; hippocampus: *sod-2*, $P \leq 0.001$; *cat*, $P \leq 0.01$; *sod-1*, *sod-3*, $P \leq 0.05$; and thalamus–hypothalamus: *cat*, $P \leq 0.001$; *sod-1*, *sod-2*, $P \leq 0.005$; *sod-3*, $P \leq 0.05$. *$P \leq 0.05$.

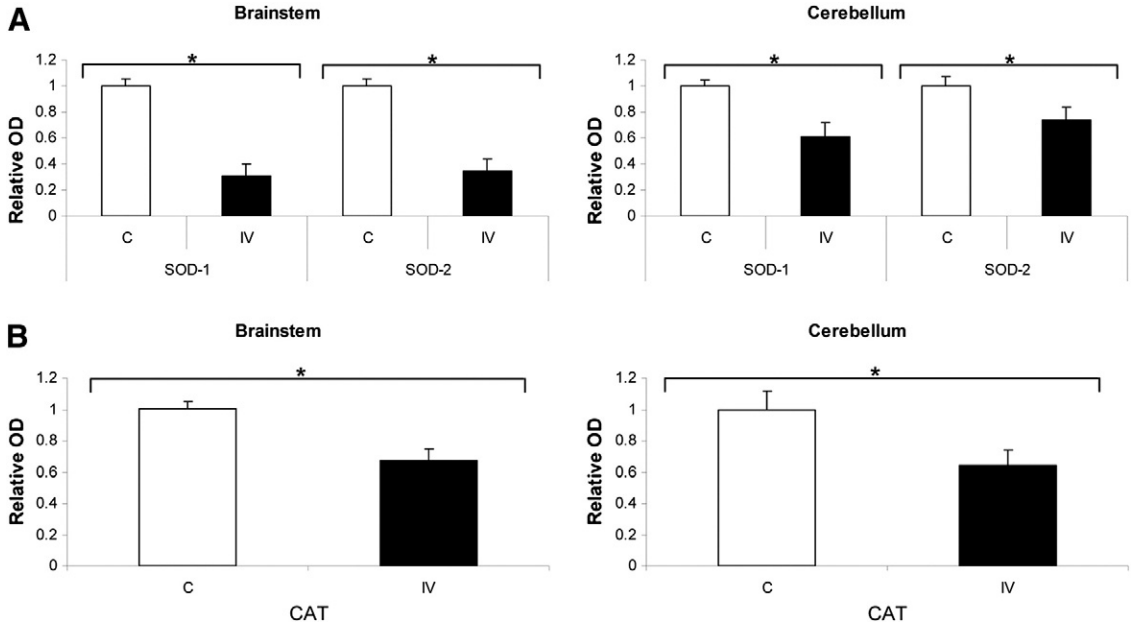

Fig. 2. Activity of SOD (panel A) and CAT (panel B) in the brainstem and cerebellum of control (C) and stage IV CM mice (IV). Values given are the mean ± standard error for 4 to 5 animals. *P* values for significant differences in SOD-1, SOD-2 and CAT activity observed in the brainstem and cerebellum, $P \leq 0.05$. $^{*}P \leq 0.05$.

3. Results

3.1. Expression of sod and cat during the clinical course of ECM

Host antioxidant systems are likely to play a major role in ROS detoxification during CM. This action especially involves removal of the superoxide radical and hydrogen peroxide by SOD and CAT. Three types of SOD isoenzymes have been identified in brain: the widely expressed cytosolic Cu/Zn-SOD (SOD-1), mitochondrial Mn-SOD (SOD-2) and copper-and zinc-extracellular SOD (SOD-3) [24,25]. To examine the roles of these enzymes during CM, mRNA expression levels of *sod-1*, *sod-2*, *sod-3* and *cat* genes were determined by qRT-PCR during the course of infection. Transcription levels of all these enzymes were significantly and steadily downregulated until stage IV, in all brain regions examined (from 2 to 4 fold depending on the region), and were most remarkably reduced in the brainstem, olfactory bulb and cerebellum (Fig. 1).

3.2. Enzyme activities of SOD and CAT in ECM

The functionality of SOD and CAT proteins was addressed by native gel electrophoresis and differential activity staining in two of the most affected regions, brainstem and cerebellum, at the most severe disease stage. These experiments revealed a band corresponding to the parasite SOD at the expected size for mammalian SOD-2 (data not shown). However, despite the possible contribution of parasite SOD activity, both SOD-1 and SOD-2 activities were significantly reduced up to 3-fold in CM stage IV, depending on the brain region examined (Fig. 2A). In parallel, CAT activity was significantly reduced up to 1.5-fold (Fig. 2B).

3.3. Expression of hsp70 and trx-1 during the clinical course of ECM

HSP are part of an extended network of stress response genes and cytoprotection genes called the vitagene system, which also includes thioredoxins. These molecules not only exert different antioxidant functions but also act as key regulators of essential cell processes [16,26,27]. Among the different TRX isoforms, the cytoplasmic TRX (TRX-1) is widely expressed in brain [16]. In this context, we examined possible vitagene system modifications during CM progression by determining *hsp70* and *trx-1* mRNA expression. Thus, *hsp70* mRNA was significantly and gradually downregulated until disease stage IV in all brain regions (from 2 to 5-fold, depending on the region) (Fig. 3A) and *trx-1* expression

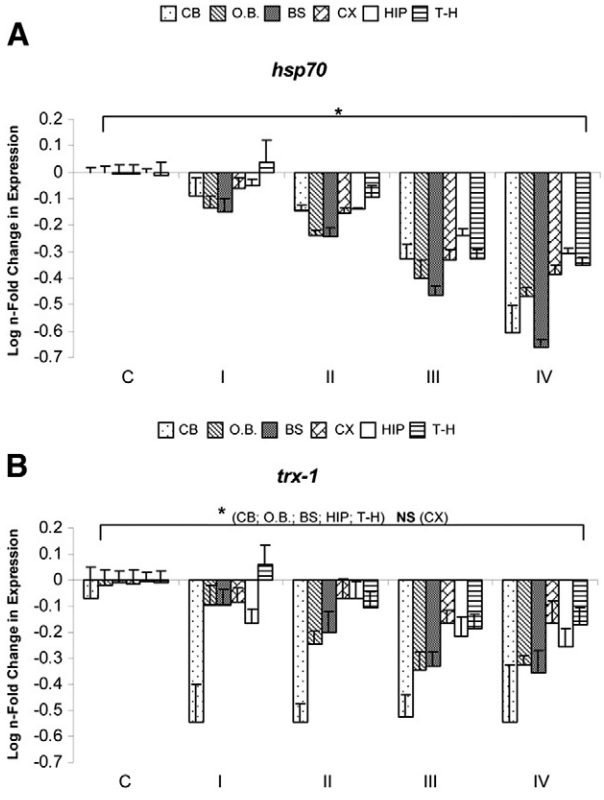

Fig. 3. Expression of *hsp70* and *trx-1* mRNA. Changes in the mRNA expression of *hsp70* (panel A) and *trx-1* (panel B) in the cerebellum (CB), olfactory bulb (O.B.), brainstem (BS), frontal cortex (CX), hippocampus (HIP) and thalamus–hypothalamus (T-H) observed in control (C) and CM mice at different disease stages (I–IV). Data are the mean ± standard error of determinations in 5–7 animals. *P* values for significant differences detected in *hsp70*: in all analyzed regions, $P \leq 0.001$; *trx-1*: in O.B., $P \leq 0.005$; BS, $P \leq 0.01$; CB, HIP, T-H, $P \leq 0.05$. $^{*}P \leq 0.05$; NS, not significant.

was also downregulated (up to 4-fold) (Fig. 3B), the reduction being significant in all regions except the frontal cortex. The two molecules were mostly downregulated in the brainstem and cerebellum.

3.4. Expression of transcription factors in brain controlling antioxidant host defenses

PARK7, XBP1 and the FOXO family of transcription factors regulate the expression of several antioxidant enzyme genes, among them SOD, CAT and TRX [28–30]. To investigate the potential role of these transcription factors (TF) in the observed downregulation of antioxidant molecules, we examined *park7*, *foxo1*, *foxo3* and *xbp1* mRNA expression. Host brain *park7*, *foxo3* and *xbp1* genes showed significant steady downregulation until stage IV up to 3-fold depending on the brain region. Again, the greatest variation was observed in the cerebellum and brainstem (Fig. 4). The *foxo1* expression pattern varied according to brain region. Thus, besides the significant gradual downregulation observed in the olfactory bulb (up to 2-fold at stage IV), an early upregulation was observed in the frontal cortex and cerebellum (up to 1.3 fold at stage II) which then decreased as neurological symptoms progressed. This pattern was only statistically significant for the cortex. Although significant changes were not observed in any other region, a downregulation tendency was observed in the brainstem, hippocampus and thalamus–hypothalamus (up to 1.5-fold at stages III–IV).

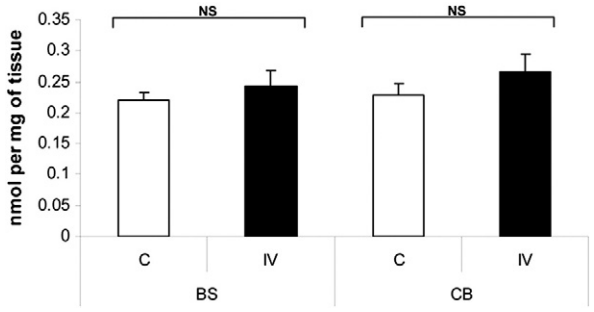

Fig. 5. Generation of ROS/RNS. Levels of ROS/RNS detected in control mice (C) and infected mice at disease stage IV (IV) in the brainstem (BS) and cerebellum (CB). Data are the mean ± standard error of determinations made in 3–5 animals calculated as nmol of ROS/RNS normalized to each milligram of tissue in each animal. NS, not significant.

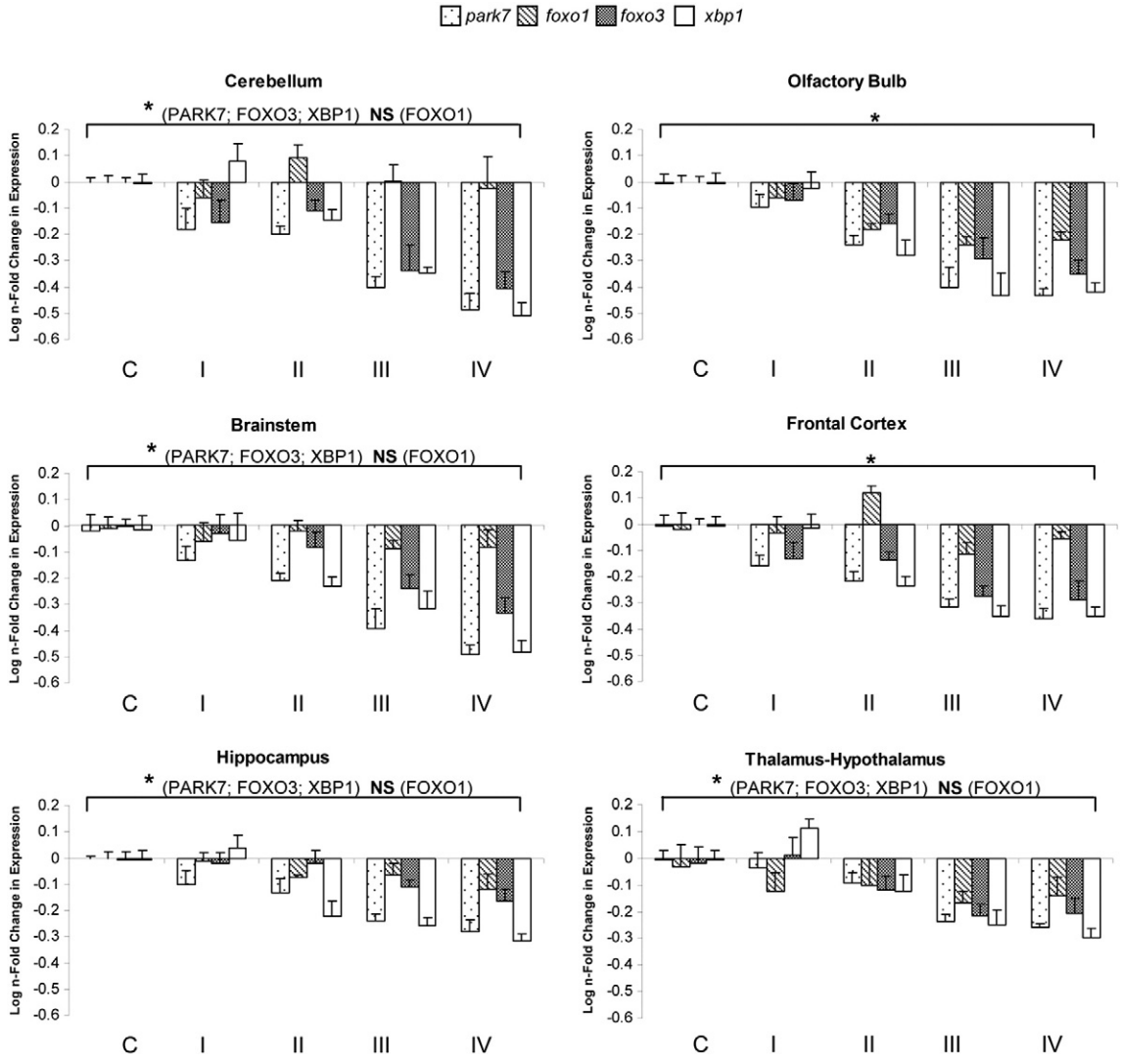

Fig. 4. mRNA expression of *park7*, *foxo1*, *foxo3* and *xbp1* in the cerebellum, olfactory bulb, brainstem, frontal cortex, hippocampus and thalamus–hypothalamus observed in control (C) and CM mice at different CM disease stages (I–IV). Data are the mean ± standard error of determinations in 5–7 animals. *P* values for significant differences detected in the cerebellum: *park7*, *xbp1*, $P \leq 0.001$; *foxo3*, $P \leq 0.005$; olfactory bulb: *park7*, *foxo1*, *xbp1*, $P \leq 0.001$; *foxo3*, $P \leq 0.005$; brainstem: *park7*, *xbp1*, $P \leq 0.001$; *foxo3*, $P \leq 0.005$; frontal cortex: *park7*, *xbp1*, $P \leq 0.001$; *foxo3*, $P \leq 0.01$; *foxo1*, $P \leq 0.05$; hippocampus: *xbp1*, $P \leq 0.001$; *park7*, $P \leq 0.005$; *foxo3*, $P \leq 0.05$; and thalamus–hypothalamus: *park7*, *xbp1*, $P \leq 0.001$; *foxo3*, $P \leq 0.05$. *$P \leq 0.05$; NS, not significant.

3.5. Reactive oxygen species production and protein carbonylation in CM

To determine if the altered levels of antioxidant proteins observed could lead to higher ROS production and intracellular oxidative stress, we quantified reactive oxygen and/or nitrogen species (ROS/RNS) and protein oxidation. ROS/RNS production (including the CAT substrate, hydrogen peroxide and the superoxide by-product, peroxynitrite anion) was evaluated in the two most affected regions, brainstem and cerebellum, at the most severe stage of infection (stage IV). However, no significant differences were observed between CM mice and uninfected animals (Fig. 5).

ROS rapidly react with protein causing protein carbonylation, which is one of the most common oxidation markers in biological systems [31]. We thus explored the carbonyl contents of individual proteins and the distribution pattern of protein carbonyls in the brains of CM mice at the most severe disease stages by 2D oxyblot and immunohistochemical

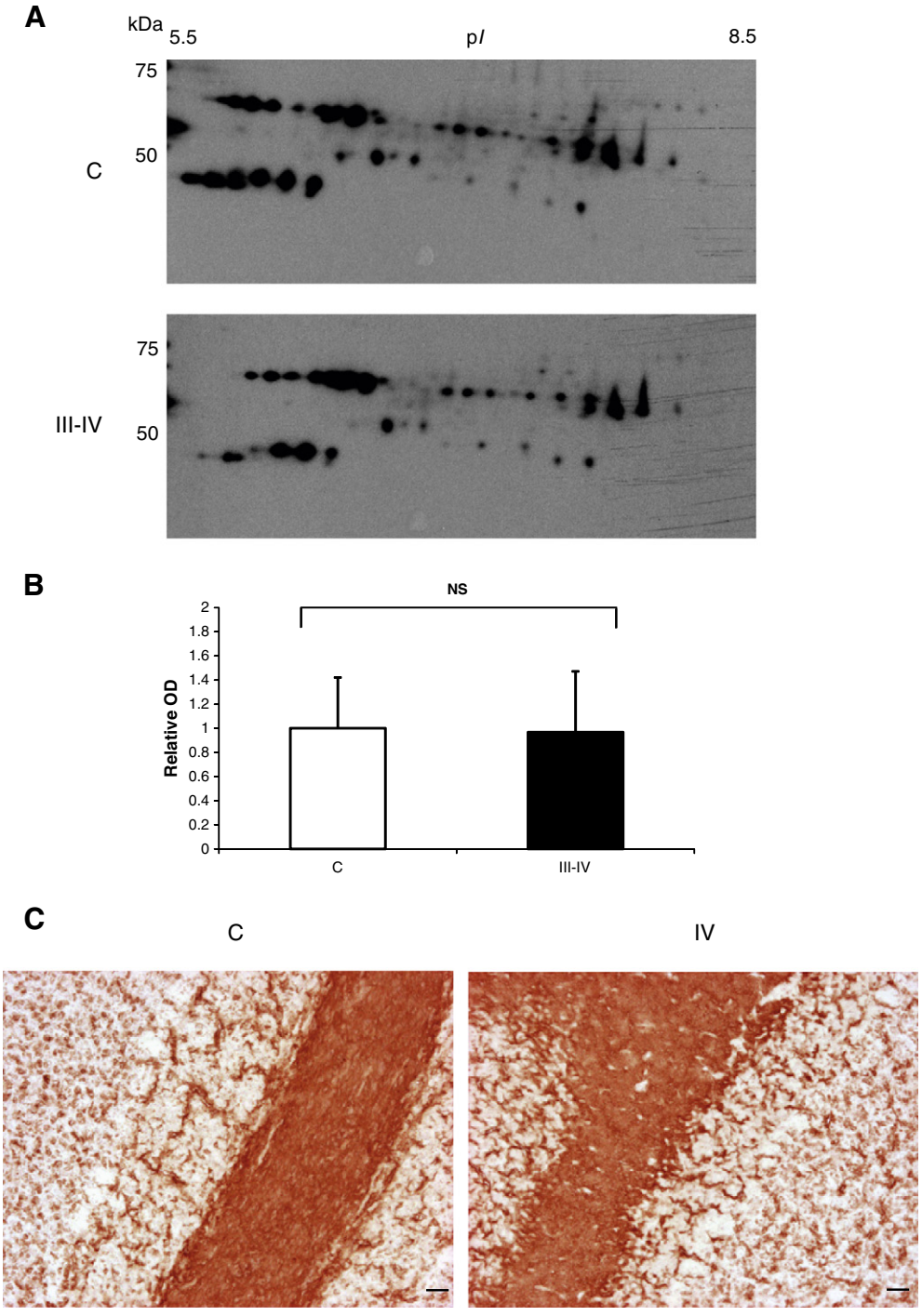

Fig. 6. Carbonyl-modified proteins: oxyblot images (panel A), total carbonyl protein content (panel B) and immunohistochemical staining of protein carbonylation (panel C). Oxyblots (panel A) and total carbonyl-modified protein content (panel B) for cerebellum specimens obtained from control (C) or infected mice at disease stages III and IV (III–IV). Images are representative of two independent experiments. Relative optical density (OD) values given are the mean ± standard error of two independent experiments using a pool of 2–3 different animals. NS, not significant. The immunohistochemical distribution profiles of protein carbonylation in brain slices (panel C) were obtained from control (C) and stage IV CM mice (IV). Images show the localization of carbonyl modified proteins in the cerebellum. Positive staining appears in dark brown color. Scale bar 50 μm.

analyses. Similar 2D oxyblot patterns and spot numbers were observed for cerebellum specimens obtained from CM or uninfected mice (Fig. 6A). Thus, between technical replicates control mice showed 69 common spots and CM samples yielded 53 common spots. More than 90% of these CM spots were also present among the spots in control mice. According to this analysis, it can be considered that protein carbonylation in brain did not vary significantly between infected and uninfected mice (Fig. 6B). To confirm this, protein carbonylation distribution patterns were investigated by immunolabelling carbonyl groups in all analyzed regions and again no differences were observed between experimental and control animals (Fig. 6C).

3.6. Expression of ho-1 and gpx-1 during the clinical course of ECM

The lack of correlation between the diminished functionality of the antioxidant systems analyzed and oxidative stress production suggests the compensatory antioxidant activity of other antioxidant systems. A protective role against ECM has been assigned to *ho-1* [32] and *gpx-1* is also an essential gene in the brain antioxidant defense [15]. Both could compensate for the partial lack of peroxide detoxification by CAT and TRX. Thus, we then examined the corresponding mRNA expression level of *ho-1* and *gpx-1* genes during CM progression. Remarkably, *ho-1* mRNA expression was progressively and significantly upregulated from disease stage 0 (controls) to IV by 7 to 37-fold depending on the brain area. The greatest expression was observed in the olfactory bulb, frontal cortex and brainstem (Fig. 7A). In contrast, the *gpx-1* expression pattern was not homogeneous across all brain regions. Thus, although significant downregulation was detected in the brainstem (up to 2-fold at stage IV), an early up-regulation was observed in most brain areas (up to 1.5-fold, depending on the region), and significantly higher *gpx-1* mRNA levels were detected in the cerebellum and thalamus–hypothalamus. Greatest increases were observed at stage II (cerebellum, frontal cortex and hippocampus) or stage I (thalamus–hypothalamus) since expression levels fell in later disease stages (Fig. 7B).

3.7. Surplus of HO-1 and GPX in ECM

According to these results, we then determined the abundance of both enzymes. HO-1 expression was analyzed by Western blot in brainstem, one of the most affected regions, at the most severe stage of the disease. This enzyme showed a significant induction by 4.5 fold in CM stage IV (Fig. 8A). On the other hand, as the greatest *gpx-1* increases were detected in cerebellum at stage II, these region and stage were chosen for GPX differential activity staining experiments. The band corresponding to GPX activity showed a significant induction by 3-fold in CM mice compared with the controls (Fig. 8B).

3.8. Expression of sod, cat, ho-1 and gpx in a non-susceptible CM model

To compare our results with a malaria mice model that does not develop the cerebral malaria syndrome, we determined, in brainstem and cerebellum, the transcription levels of the most significant enzyme markers in BALB/c mice infected with *P. berghei* ANKA. We did not observe any change between infected and controls in the *gpx* and *sod-3* expression in both brain regions analyzed. *cat* and *ho-1* did not change mRNA expression levels in brainstem but a minor variation was detected in cerebellum. On the other hand, *sod-1* and *sod-2* were slightly downregulated in both regions, ranging from 1.3 to 2.0 fold (Table 1). When changes were detected, they were notably lower than those observed for these genes in CM susceptible mice.

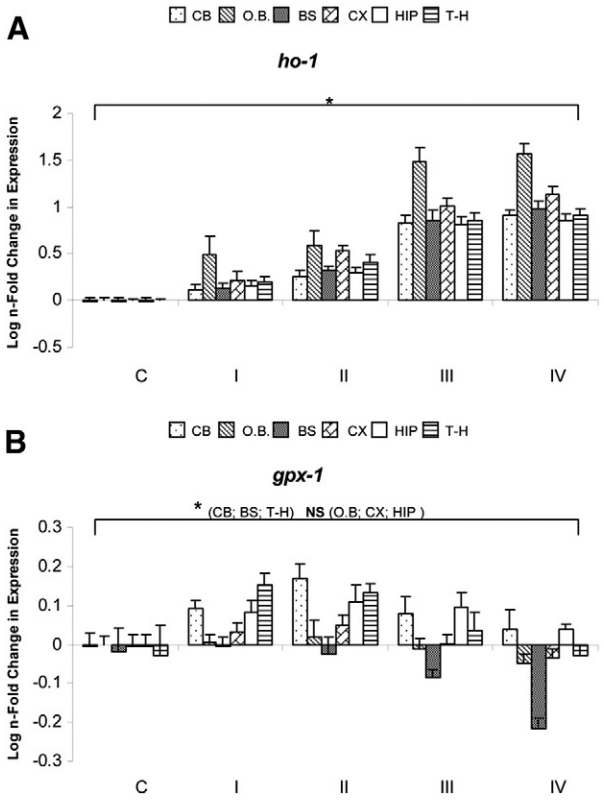

Fig. 7. mRNA expression of *ho-1* (panel A) and *gpx-1* (panel B) in the cerebellum (CB), olfactory bulb (O.B.), brainstem (BS), frontal cortex (CX), hippocampus (HIP) and thalamus–hypothalamus (T-H) detected in control mice (C) and CM mice at different disease stages (I–IV). Data are the mean ± standard error of determinations in 5–7 animals. *P* values for significant differences detected in *ho-1*: in all analyzed regions, $P \leq 0.001$; and *gpx-1*: in BS, $P \leq 0.005$; CB, T-H, $P \leq 0.05$. $^{*}P \leq 0.05$; NS, not significant.

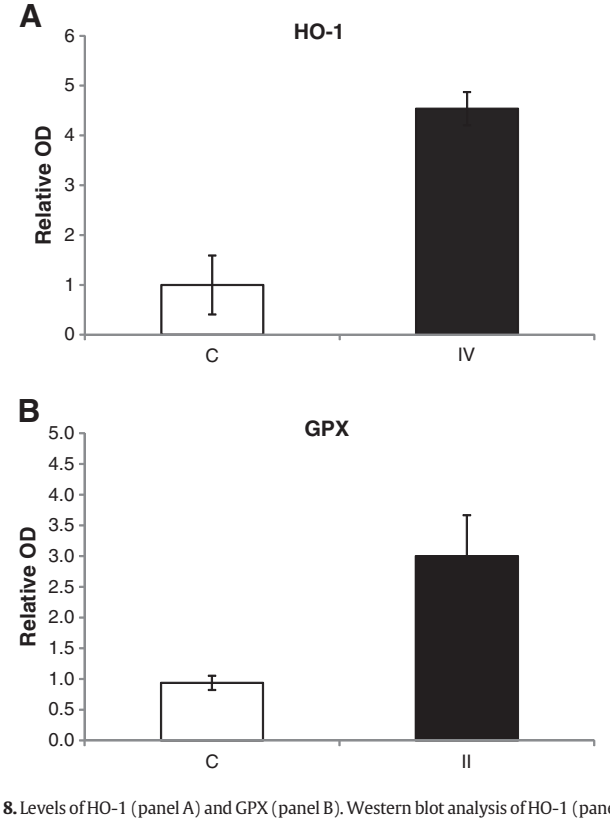

Fig. 8. Levels of HO-1 (panel A) and GPX (panel B). Western blot analysis of HO-1 (panel A) in the brainstem of control (C) and infected mice at stage IV (IV). Anti-GADPH antibody was used to demonstrate equal loading of protein samples. Relative optical density (OD) values given are the mean ± standard error for determinations in 4–5 animals. Activity analysis of GPX activity (panel B) in the cerebellum of control (C) and stage II CM mice (II). Values given are the mean ± standard error for 4 animals. *P* values for significant differences in HO-1 expression and GPX activity, $P \leq 0.05$. $^{*}P \leq 0.05$.

Table 1
Comparison of mRNA expression in brainstem and cerebellum of infected BALB/c and C57BL/6 mice. N-fold changes are the mean ± standard error of determinations in 4–7 animals. *P* values for significant differences detected in mRNA expression analysis in BALB/c in brainstem: *sod-1*, $P \leq 0.01$; *sod-2*, $P \leq 0.05$; cerebellum: *sod-2*, *cat* and *ho-1*, $P \leq 0.01$; *sod-1*: $P \leq 0.05$; C57BL/6-II in brainstem: *sod-2* and *ho-1*, $P \leq 0.005$; *sod-1*, $P \leq 0.05$; in cerebellum: *gpx-1*, $P \leq 0.01$; *sod-2* and *ho-1*, $P \leq 0.05$; C57BL/6-IV in brainstem: *sod-1*, *sod-2*, *sod-3*, *cat* and *ho-1*: $P \leq 0.005$; *gpx-1*: $P \leq 0.01$; cerebellum: *sod-1*, *sod-2*, *cat* and *ho-1*: $P \leq 0.005$; sod-3: $P \leq 0.05$. Asterisk (*) indicates significant differences ($P \leq 0.05$) with respect to the corresponding healthy control strain.

Gene	BALB/c	C57BL/6-II	C57BL/6-IV	Ratio	
				C57BL/6-II vs. BALB/c	C57BL/6-IV vs. BALB/c
Brainstem					
sod-1	−0.248* ± 0.041	−0.157* ± 0.032	−0.397* ± 0.039	1	2
sod-2	−0.107* ± 0.023	−0.234* ± 0.033	−0.572* ± 0.034	2	5
sod-3	−0.021 ± 0.039	−0.060 ± 0.045	−0.304* ± 0.046	3	14
cat	−0.010 ± 0.020	−0.153 ± 0.064	−0.484* ± 0.046	16	50
ho-1	0.008 ± 0.013	0.322* ± 0.048	0.980* ± 0.090	40	122
gpx-1	−0.013 ± 0.023	−0.025 ± 0.044	−0.216* ± 0.027	2	16
Cerebellum					
sod-1	−0.129* ± 0.017	−0.056 ± 0.033	−0.287* ± 0.045	0	2
sod-2	−0.231* ± 0.042	−0.128* ± 0.024	−0.344* ± 0.052	1	1
sod-3	0.008 ± 0.046	0.043 ± 0.039	−0.257* ± 0.060	6	−34
cat	−0.192* ± 0.014	−0.072 ± 0.035	−0.329* ± 0.057	0	2
ho-1	0.215* ± 0.043	0.254* ± 0.070	0.907* ± 0.056	1	4
gpx-1	0.076 ± 0.024	0.170* ± 0.036	0.040 ± 0.050	2	1

3.9. Abundance of SOD, CAT and HO-1 in a non-susceptible CM model

According to the above results, we then determined the abundance of SOD-1, SOD-2, CAT and HO-1 in cerebellum, since it was the most affected region. None of these enzymes presented any change in terms of protein activity or expression, respectively (Table 2). In addition, we corroborated the absence of changes in the enzyme activity of GPX in cerebellum and SOD-1 and SOD-2 in brainstem (data not shown).

4. Discussion

The generation of local oxidative stress factors during cerebral malaria is still a matter of debate. Further, there is no general consensus as to the precise role played by oxidative stress in CM. To address the oxidative stress status of the infected host brain and its implications in the neurocognitive damage produced by cerebral malaria, we examined a broad set of oxidative stress markers and antioxidant defense systems in host brain regions during the course of ECM.

In this experimental setting, we observed the functional failure of host antioxidant defense system at the level of superoxide dismutase and catalase enzyme activities in brain. Moreover, at the mRNA level, the significantly and gradually reduced expression of the three *sod* isoenzymes and *cat* genes was seen to parallel the progression of neurological symptoms. Both SOD and CAT mediate neuroprotective effects [24,33]. Altered expression levels and diminished activity of these two enzymes have been reported in other neurological disorders [24,34,35]. Further, low levels of both enzymes have also been detected in blood of human malaria patients [7,36]. In experimental mouse models, treatment with SOD or CAT prolongs survival or prevents CM [5,12,24].

The SOD and CAT alterations detected in this study could be explained, at least in part, by the *hsp70* significant downregulation observed during CM progression. The inducible chaperone HSP 70 regulates the enzymatic activities of SOD-1, SOD-2 and CAT [26,37] and also plays a role in neuroprotection through an array of pro-survival effects [16,26,38]. TRX-1 is another component of the host antioxidant defense system which reduces peroxides and disulfide bridges in proteins in concert with peroxyredoxins and TRX reductases and acts alone as an antioxidant or ROS scavenger [16,27]. During the progression of ECM, in parallel with *cat*, *sod* and *hsp70* downregulation, *trx-1* expression was also significantly reduced. Diminished TRX-1 levels have been observed in the brains of patients with Alzheimer's disease [27] and their upregulation has been linked to neuron survival following injury [16].

Table 2
Comparison of enzyme activity of SOD-1, SOD-2 and CAT and protein expression of HO-1 in cerebellum of infected BALB/c and C57BL/6 mice. Relative values given are the mean ± standard error in 4–5 animals. *P* values for significant differences in SOD-1, SOD-2, CAT and HO-1 observed in C57BL/6, $P \leq 0.05$. Asterisk (*) indicates significant differences ($P \leq 0.05$) with respect to the corresponding healthy control strain. ND, not determined.

Protein	BALB/c	C57BL/6
SOD-1	1.130 ± 0.068	0.611* ± 0.109
SOD-2	1.095 ± 0.114	0.737* ± 0.099
CAT	0.892 ± 0.267	0.639* ± 0.100
HO-1	1.150 ± 0.124	>5* ± ND

Thus, all these antioxidant molecules promote neuroprotection in brain and their deficiency could lead to the neurodegeneration produced in CM. These changes observed in these molecules could explain why antioxidants protect against CM [6,12,13] and suggest the use of these antioxidant molecules as complementary therapeutic agents for the management of cerebral malaria and to reduce its neurological sequelae. On the other hand, among the differences in local antioxidant responses observed in the present study, the brainstem and cerebellum were the most affected regions, as previously detected for other dysfunctional factors [17,18]. Alterations in these specific regions could explain some of CM's symptoms and sequelae, such as ataxia and impaired movement and balance [1,3].

In the last 20 years, a number of transcription factors that mediate critical transcription responses to oxidative stress have been identified [39]. Thus, PARK7, XBP1 and the FOXO family of transcription factors regulate several antioxidant related genes [28–30]. In our study, the expression of *foxo3*, *xbp1* and *park7* was significantly downregulated in all the brain regions and, in general, *foxo1* also showed this tendency. Therefore, the mechanism underlying reduced antioxidant gene expression during CM appears to be related to a decline in these TF. FOXO upregulates *sod-2* and *cat* expression [39,40], *xbp1* knockdown has been found to decrease *cat*, *sod-1* and *trx-1* expression [29] and PARK 7, that could act as an antioxidant protein [41], can also modulate HSP70 and SOD-1 [42,43].

Uncontrolled oxidative stress could damage host antioxidant defenses [5]. Hence, we examined ROS production and protein carbonylation, as markers of oxidative stress. Oxidative stress has been observed in pRBC by *P. falciparum* and *P. berghei* [5,10,11]. In addition, cerebral malaria causes lipid peroxidation to a greater extent in human cerebrospinal fluid [44] than in mouse brain [6]. However, we were unable to detect differences in the accumulation of ROS in mice brain with severe stage CM and uninfected controls. ROS rapidly react with proteins causing carbonylation. Nevertheless, neither the level of protein carbonylation nor its

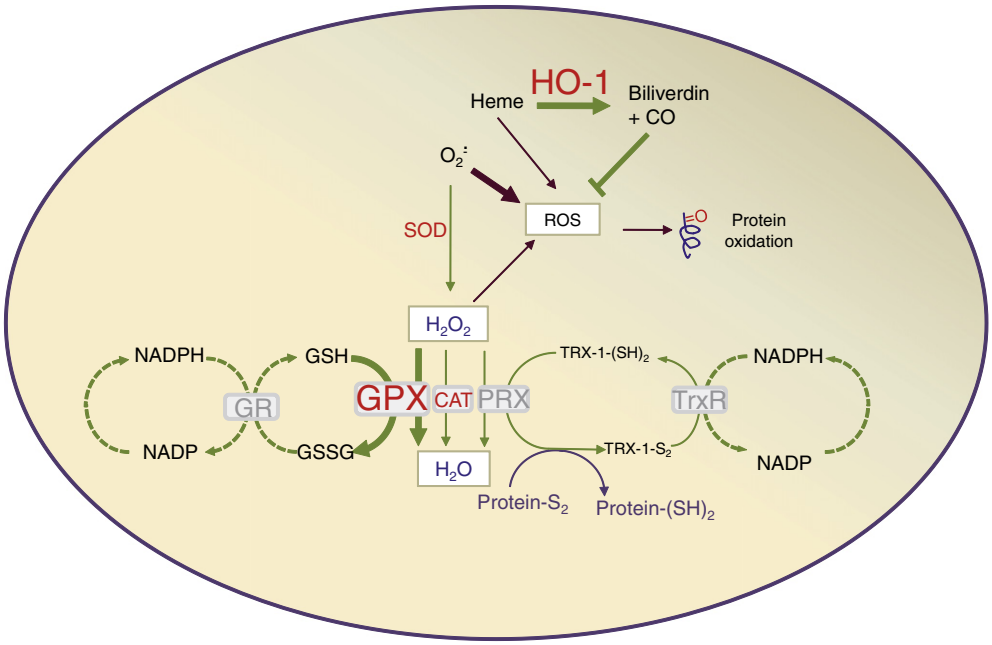

Fig. 9. Redox regulation during ECM progression. The cartoon summarizes the hypothetical adaptation of redox systems during ECM. The diminished expression of SOD, CAT, TRX-1 (and HSP70: not depicted) is compensated in all cerebral regions by the induction of HO-1 and GPX. Reactions with oxidative effects are indicated as purple arrows whereas reactions with antioxidant effects are shown by green arrows. Letter-font size of abbreviated enzymes and line thickness of reaction arrows are associated with their corresponding up- or downregulation. GPR, glutathione reductase; PRX, peroxiredoxin; TRX-r, thioredoxin reductase.

distribution pattern in the brain of CM mice differed from those detected in the brain of control mice. The lack of alterations in total protein carbonyl contents in CM has been reported [14], and along with our results suggests that ROS overproduction, if present, is well controlled in ECM and plays no major role in its pathogenesis. On the other hand, given the oxidative modification of proteins predisposes them to proteolysis, some increased protein carbonylation might not be readily detected [14].

Globally, our results could also be explained by the compensatory induction of *ho-1* and *gpx-1* genes in several brain regions (Fig. 9). HO-1 production seems to be one of the earlier cellular responses to tissue damage [16]. Bilirubin, one of the final products of heme degradation by HO-1, protects against the cytotoxic effects of the strong oxidants hydrogen peroxide and peroxynitrite [16,45,46]. Carbon monoxide, another by-product of the actions of HO-1, limits the production of free heme, exerts anti-inflammatory actions [45] and suppresses the pathogenesis of cerebral malaria in mice [32,47]. Increased levels of HO-1 have been previously observed in CM as well as in other neurological diseases [16,48,49]. On the other hand, GPX reduces hydrogen peroxide and organic hydroperoxides [15]. As mentioned above, *xbp1* deletion reduces several antioxidant enzymes but not *gpx* expression [29], supporting the different *gpx-1* expression pattern observed in our ECM model. Elevated GPX activity has been observed in other neurological diseases such as Alzheimer's [16] but, until now, its induction in CM had not been described.

In this study, the changes observed in the analyzed redox markers seem to be related to the cerebral syndrome of murine malaria. In a non-cerebral malaria model (BALB/c infected with *P. berghei* ANKA), only some of the markers analyzed showed minor changes in comparison to the changes observed in ECM. Moreover, those were not translated into protein content or enzymatic activity. In addition these fluctuations seem to be dependent on the brain region.

5. Conclusions

In conclusion, these observations suggest a central role of antioxidant systems during the progress of cerebral malaria which is not accompanied by the build-up of oxidative stress metabolites. The changes observed in these systems during the course of CM open new perspectives for the treatment of this disease. The pharmacological or nutritional manipulation of endogenous cellular defense mechanisms is an innovative approach to therapeutic intervention [16]. In this context, the recently reported protective effect of curcumin against ECM [50] could be mediated by inducing the heat-shock response coupled to other antioxidant activities [16].

List of abbreviations

BLAST	basic local alignment search tool;
CAT	catalase;
CHAPS	3-[(3-cholamidopropyl) dimethylammonio]-1-propanesulfonate;
CM	cerebral malaria;
DNP	2,4-dinitrophenylhydrazone;
ECM	experimental cerebral malaria;
FOXO	Forkhead box O;
GADPH	glyceraldehyde 3-phospate dehydrogenase;
GPX	glutathione peroxidase;
GPR	glutathione reductase;
HO	heme oxygenase;
HSP	heat shock protein;
IEF	isoelectric focusing;
IPG	immobilized pH gradient;
PARK7	Parkinson disease 7;
pRBC	parasitized red blood cells;
PRX	peroxiredoxin
PVDF	polyvinylidene fluoride;
qRT-PCR	quantitative reverse transcriptase-PCR;
RNS	reactive nitrogen species;
ROS	reactive oxygen species;
SDS	sodium lauryl sulfate;
SOD	superoxide dismutase;
TCA	trichloroacetic acid;
TF	transcription factor;
TRX	thioredoxin;
TRX-r	thioredoxin reductase;
XBP1	X-box binding protein 1.

Gene names appear as low-case italics of the corresponding protein abbreviations specified above.

Acknowledgements

This work was supported by grant BIO2010-17039 from the Spanish Ministry of Education and Science and by the Research Teams Consolidation Programme of the UCM (Research Team 920267-Comunidad de Madrid). M.L. holds a FPU fellowship from the Spanish Ministry of Education and Science (AP20061576). We are particularly indebted to Drs. Montserrat Martínez-Gomariz and Marisol Fernández from the Proteomics Facilities UCM-PCM and CNB-PCM, respectively (components of the ProteoRed Network). We thank Ana Burton for reviewing the English and commenting on the manuscript.

References

[1] R. Idro, K. Marsh, C.C. John, C.R. Newton, Cerebral malaria: mechanisms of brain injury and strategies for improved neurocognitive outcome, Pediatr. Res. 68 (2010) 267–274.
[2] WHO, World Malaria Report 2011, World Health Organization, 2011. (http://www.who.int/malaria/world_malaria_report_2011/en/).
[3] M.J. Boivin, P. Bangirana, J. Byarugaba, R.O. Opoka, R. Idro, A.M. Jurek, C.C. John, Cognitive impairment after cerebral malaria in children: a prospective study, Pediatrics 119 (2007) e360–e366.
[4] P. Pino, Z. Taoufiq, J. Nitcheu, I. Vouldoukis, D. Mazier, Blood-brain barrier breakdown during cerebral malaria: suicide or murder? Thromb. Haemost. 94 (2005) 336–340.
[5] N.S. Postma, E.C. Mommers, W.M. Eling, J. Zuidema, Oxidative stress in malaria; implications for prevention and therapy, Pharm. World Sci. 18 (1996) 121–129.
[6] P.A. Reis, C.M. Comim, F. Hermani, B. Silva, T. Barichello, A.C. Portella, F.C. Gomes, I.M. Sab, V.S. Frutuoso, M.F. Oliveira, P.T. Bozza, F.A. Bozza, F. Dal-Pizzol, G.A. Zimmerman, J. Quevedo, H.C. Castro-Faria-Neto, Cognitive dysfunction is sustained after rescue therapy in experimental cerebral malaria, and is reduced by additive antioxidant therapy, PLoS Pathog. 6 (2010) e1000963.
[7] K. Becker, L. Tilley, J.L. Vennerstrom, D. Roberts, S. Rogerson, H. Ginsburg, Oxidative stress in malaria parasite-infected erythrocytes: host–parasite interactions, Int. J. Parasitol. 34 (2004) 163–189.
[8] N.H. Hunt, J. Golenser, T. Chan-Ling, S. Parekh, C. Rae, S. Potter, I.M. Medana, J. Miu, H.J. Ball, Immunopathogenesis of cerebral malaria, Int. J. Parasitol. 36 (2006) 569–582.
[9] C. Nickel, S. Rahlfs, M. Deponte, S. Koncarevic, K. Becker, Thioredoxin networks in the malarial parasite *Plasmodium falciparum*, Antioxid. Redox Signal. 8 (2006) 1227–1239.
[10] D. Mendez, M. Linares, A. Diez, A. Puyet, J.M. Bautista, Stress response and cytoskeletal proteins involved in erythrocyte membrane remodeling upon *Plasmodium falciparum* invasion are differentially carbonylated in G6PD A(−) deficiency, Free Radic. Biol. Med. 50 (2011) 1305–1313.
[11] A. Radfar, A. Diez, J.M. Bautista, Chloroquine mediates specific proteome oxidative damage across the erythrocytic cycle of resistant *Plasmodium falciparum*, Free Radic. Biol. Med. 44 (2008) 2034–2042.
[12] Z. Taoufiq, P. Pino, N. Dugas, M. Conti, M. Tefit, D. Mazier, I. Vouldoukis, Transient supplementation of superoxide dismutase protects endothelial cells against *Plasmodium falciparum*-induced oxidative stress, Mol. Biochem. Parasitol. 150 (2006) 166–173.
[13] I. Vouldoukis, D. Lacan, C. Kamate, P. Coste, A. Calenda, D. Mazier, M. Conti, B. Dugas, Antioxidant and anti-inflammatory properties of a *Cucumis melo* L.C. extract rich in superoxide dismutase activity, J. Ethnopharmacol. 94 (2004) 67–75.
[14] L.A. Sanni, S. Fu, R.T. Dean, G. Bloomfield, R. Stocker, G. Chaudhri, M.C. Dinauer, N.H. Hunt, Are reactive oxygen species involved in the pathogenesis of murine cerebral malaria? J. Infect. Dis. 179 (1999) 217–222.
[15] R. Dringen, P.G. Pawlowski, J. Hirrlinger, Peroxide detoxification by brain cells, J. Neurosci. Res. 79 (2005) 157–165.
[16] V. Calabrese, E. Guagliano, M. Sapienza, M. Panebianco, S. Calafato, E. Puleo, G. Pennisi, C. Mancuso, D.A. Butterfield, A.G. Stella, Redox regulation of cellular stress response in aging and neurodegenerative disorders: role of vitagenes, Neurochem. Res. 32 (2007) 757–773.
[17] M. Linares, P. Marín-García, S. Pérez-Benavente, J. Sánchez-Nogueiro, A. Puyet, J.M. Bautista, A. Diez, Brain-derived neurotrophic factor and the course of experimental cerebral malaria, Brain Res. 1490 (2013) 210–224.
[18] P. Marin-Garcia, J. Sanchez-Nogueiro, A. Diez, M. Leon-Otegui, M. Linares, P. Garcia-Palencia, J.M. Bautista, M.T. Miras-Portugal, Altered nucleotide receptor expression in a murine model of cerebral malaria, J. Infect. Dis. 200 (2009) 1279–1288.
[19] M. Li, J.F. Chiu, B.T. Mossman, N.K. Fukagawa, Down-regulation of manganese-superoxide dismutase through phosphorylation of FOXO3a by Akt in explanted vascular smooth muscle cells from old rats, J. Biol. Chem. 281 (2006) 40429–40439.
[20] C.L. Lin, H.J. Chen, W.C. Hou, Activity staining of glutathione peroxidase after electrophoresis on native and sodium dodecyl sulfate polyacrylamide gels, Electrophoresis 23 (2002) 513–516.
[21] H. Tayefi-Nasrabadi, Some biochemical properties of catalase from kohlrabi (*Brassica oleracea gogylodes*), J. Biol. Sci. 8 (2008) 5.
[22] M. Linares, P. Marin-Garcia, D. Mendez, A. Puyet, A. Diez, J.M. Bautista, Proteomic approaches to identifying carbonylated proteins in brain tissue, J. Proteome Res. 10 (2011) 1719–1727.
[23] J. Frank, A. Pompella, H.K. Biesalski, Immunohistochemical detection of protein oxidation, Methods Mol. Biol. 196 (2002) 35–40.
[24] C.M. Maier, P.H. Chan, Role of superoxide dismutases in oxidative damage and neurodegenerative disorders, Neuroscientist 8 (2002) 323–334.
[25] T. Ookawara, N. Imazeki, O. Matsubara, T. Kizaki, S. Oh-Ishi, C. Nakao, Y. Sato, H. Ohno, Tissue distribution of immunoreactive mouse extracellular superoxide dismutase, Am. J. Physiol. 275 (1998) C840–C847.
[26] S. Choi, K.A. Park, H.J. Lee, M.S. Park, J.H. Lee, K.C. Park, M. Kim, S.H. Lee, J.S. Seo, B.W. Yoon, Expression of Cu/Zn SOD protein is suppressed in hsp 70.1 knockout mice, J. Biochem. Mol. Biol. 38 (2005) 111–114.
[27] A. Patenaude, M.R. Murthy, M.E. Mirault, Emerging roles of thioredoxin cycle enzymes in the central nervous system, Cell. Mol. Life Sci. 62 (2005) 1063–1080.
[28] P.J. Kahle, J. Waak, T. Gasser, DJ-1 and prevention of oxidative stress in Parkinson's disease and other age-related disorders, Free Radic. Biol. Med. 47 (2009) 1354–1361.
[29] Y. Liu, M. Adachi, S. Zhao, M. Hareyama, A.C. Koong, D. Luo, T.A. Rando, K. Imai, Y. Shinomura, Preventing oxidative stress: a new role for XBP1, Cell Death Differ. 16 (2009) 847–857.
[30] P. Storz, Forkhead homeobox type O transcription factors in the responses to oxidative stress, Antioxid. Redox Signal. 14 (2011) 593–605.
[31] R.L. Levine, J.A. Williams, E.R. Stadtman, E. Shacter, Carbonyl assays for determination of oxidatively modified proteins, Methods Enzymol. 233 (1994) 346–357.
[32] A. Pamplona, A. Ferreira, J. Balla, V. Jeney, G. Balla, S. Epiphanio, A. Chora, C.D. Rodrigues, I.P. Gregoire, M. Cunha-Rodrigues, S. Portugal, M.P. Soares, M.M. Mota, Heme oxygenase-1 and carbon monoxide suppress the pathogenesis of experimental cerebral malaria, Nat. Med. 13 (2007) 703–710.
[33] T. Gaspar, F. Domoki, L. Lenti, A. Institoris, J.A. Snipes, F. Bari, D.W. Busija, Neuroprotective effect of adenoviral catalase gene transfer in cortical neuronal cultures, Brain Res. 1270 (2009) 1–9.
[34] D.L. Marcus, C. Thomas, C. Rodriguez, K. Simberkoff, J.S. Tsai, J.A. Strafaci, M.L. Freedman, Increased peroxidation and reduced antioxidant enzyme activity in Alzheimer's disease, Exp. Neurol. 150 (1998) 40–44.
[35] J.K. Yao, R. Reddy, Oxidative stress in schizophrenia: pathogenetic and therapeutic implications, Antioxid. Redox Signal. 15 (2011) 1999–2002.
[36] N. Narsaria, C. Mohanty, B.K. Das, S.P. Mishra, R. Prasad, Oxidative stress in children with severe malaria, J. Trop. Pediatr. 58 (2011) 147–150.
[37] C. Romero, J. Benedi, A. Villar, S. Martin-Aragon, Involvement of Hsp70, a stress protein, in the resistance of long-term culture of PC12 cells against sodium nitroprusside (SNP)-induced cell death, Arch. Toxicol. 84 (2010) 699–708.
[38] R.G. Giffard, R.Q. Han, J.F. Emery, M. Duan, J.F. Pittet, Regulation of apoptotic and inflammatory cell signaling in cerebral ischemia: the complex roles of heat shock protein 70, Anesthesiology 109 (2008) 339–348.
[39] Q. Ma, Transcriptional responses to oxidative stress: pathological and toxicological implications, Pharmacol. Ther. 125 (2010) 376–393.
[40] G.J. Kops, T.B. Dansen, P.E. Polderman, I. Saarloos, K.W. Wirtz, P.J. Coffer, T.T. Huang, J.L. Bos, R.H. Medema, B.M. Burgering, Forkhead transcription factor FOXO3a protects quiescent cells from oxidative stress, Nature 419 (2002) 316–321.
[41] B. Thomas, M.F. Beal, Parkinson's disease, Hum. Mol. Genet. 16 (Spec No. 2) (2007) R183–R194.
[42] X.M. Xu, H. Lin, J. Maple, B. Bjorkblom, G. Alves, J.P. Larsen, S.G. Moller, The *Arabidopsis* DJ-1a protein confers stress protection through cytosolic SOD activation, J. Cell Sci. 123 (2010) 1644–1651.
[43] W. Zhou, K. Bercury, J. Cummiskey, N. Luong, J. Lebin, C.R. Freed, Phenylbutyrate upregulates DJ-1 and protects neurons in cell culture and in animal models of Parkinson's disease, J. Biol. Chem. 286 (2011) 14941–14951.
[44] B.S. Das, S. Mohanty, S.K. Mishra, J.K. Patnaik, S.K. Satpathy, D. Mohanty, T.K. Bose, Increased cerebrospinal fluid protein and lipid peroxidation products in patients with cerebral malaria, Trans. R. Soc. Trop. Med. Hyg. 85 (1991) 733–734.
[45] N.H. Hunt, R. Stocker, Heme moves to center stage in cerebral malaria, Nat. Med. 13 (2007) 667–669.
[46] G.G. van Dooren, A.T. Kennedy, G.I. McFadden, The use and abuse of heme in apicomplexan parasites, Antioxid. Redox Signal. 17 (2012) 634–656.
[47] A.C. Pena, N. Penacho, L. Mancio-Silva, R. Neres, J.D. Seixas, A.C. Fernandes, C.C. Romao, M.M. Mota, G.J. Bernardes, A. Pamplona, A novel carbon monoxide-releasing molecule fully protects mice from severe malaria, Antimicrob. Agents Chemother. 56 (2012) 1281–1290.
[48] M.S. Oakley, T.F. McCutchan, V. Anantharaman, J.M. Ward, L. Faucette, C. Erexson, B. Mahajan, H. Zheng, V. Majam, L. Aravind, S. Kumar, Host biomarkers and biological pathways that are associated with the expression of experimental cerebral malaria in mice, Infect. Immun. 76 (2008) 4518–4529.
[49] H.J. Schluesener, P.G. Kremsner, R. Meyermann, Heme oxygenase-1 in lesions of human cerebral malaria, Acta Neuropathol. 101 (2001) 65–68.
[50] J.H. Waknine-Grinberg, J.A. McQuillan, N. Hunt, H. Ginsburg, J. Golenser, Modulation of cerebral malaria by fasudil and other immune-modifying compounds, Exp. Parasitol. 125 (2010) 141–146.